MUUFL Gulfport

Hyperspectral and LiDAR Airborne Data Set

Paul Gader, University of Florida
Alina Zare, University of Missouri
Ryan Close, University of Florida
Jen Aitken, Optech, International
Grady Tuell, Optech, International

1 Abstract

An airborne data collection was conducted in November 2010. Data were collected using a Gemini LiDAR and CASI-1500 flown in a single plane simultaneously, thereby provided co-registered hyperspectral and LiDAR data. The collection was designed to support general, open research. Sixty-four cloths with various spectral characteristics were acquired and used to construct super-pixel and sub-pixel targets. They were placed on the campus of the University of Southern Mississippi – Gulfport, located in Long Beach, Mississippi (close to Gulfport, MS). The level of target occlusion ranged from almost completely occluded to non-occluded. The airborne measurements were taken by Optech, International, with support from 3001, Inc. The collection is described in this document.

2 Data Collection

The collection was designed to support our research goals as well as providing a general, open data set that could be used by others. The measurement process was conducted by Optech, International, which is located in Kiln, Mississippi (close to Gulfport, MS). The collection is described in this chapter of the report.

The desired characteristics of the data collection were as follows:
Data Collection Desired Characteristics

(1) Well defined regions for ground truth
(2) Tree canopy
(3) Slowly varying ground covers
(4) Easy access
(5) No restrictions

(6) GPS coordinates of targets, trees, boundaries
(7) Heights of targets and other objects in the scene
(8) Small number of target object types
(9) Significant regions with no targets
(10) Variation in target spectra, Easy to difficult targets to distinguish spectrally.
(11) Variation in target size, subpixel to multi-pixel.
(12) Excellent weather conditions

The steps involved in the collection and subsequent data preparation were as follows:

Site Selection
Target Selection
Target Construction
Target Emplacement
Ground Measurements
Airborne Measurements
Post-processing
Ground-Truthing

These steps are each described in the following sections.

2.1 Site Selection

The site was chosen in the vicinity of Optech, International because there is an airstrip nearby so the costs were lowest. After investigating several sites in the area, the campus of the University of Southern Mississippi – Gulfport, located in Long Beach, MS, was chosen. The campus is pictured in Figure 1. The address is:

University of Southern Mississippi Long Beach
730 E Beach Blvd
Long Beach, MS

Figure 2-1: University of Southern Mississippi Long Beach

This choice of site allowed the data collection to include a variety of ground cover types such as water, beach, sand, grass, tree, road, dead vegetation, and dirt. Some examples of these ground cover types are shown in Figure 2. In addition to the varied ground cover, this site offered a variety of geographical features and scene elements such as flat fields, wooded areas, buildings (buildings in use and buildings condemned from hurricane damage), roads, and a stream. This scene also provided a plethora of indigenous targets, to include among others, concrete tables, pillars, cars, and sidewalks, some of which are pictured in Figure 3. The combination of these natural scene elements allowed for a rich mixture of targets, contexts, and features to be collected.

Figure 2-2: Example of four ground cover types present in the scene

Figure 2-3: Example of indigenous targets

Another advantage of this site for the data collection was the tree canopy provided by the Live Oaks present on the campus. The density of the tree canopy varied with the age of the Live Oaks forming it. The varying density of the tree canopy (shown in Figure 4) allowed us to position identical targets (described in Section B) in areas of:

- Predominate tree coverage
- Partial tree occlusion
- Low light due to shadow
- Open field

Using identical targets under varied light and occlusion conditions will allow qualitative and quantitative analysis of the capabilities of the algorithms being investigated.

Figure 2-4: Representative examples of canopy cover

2.2 Target Selection and Construction

The site chosen for the data collection included a variety of static targets. However, in order to perform a robust and statistically rigorous experiment, targets were designed that met an exact set of parameters and could be replicated for use in a variety of collection conditions to test the effects of lighting and tree occlusion. To this end the targets needed to be designed in such a way as to conform to a principled experimental setup and simultaneously provide sufficient difficulty in detection so as to replicate operational characteristics. The following subsections describe the parameters considered for the targets construction and how our targets conform to these parameters.

1) Target Construction.

After much discussion, 64 targets were constructed. These targets fell into two categories, those used for evaluating endmember detection, pixel unmixing and target detection techniques and those used for evaluating atmospheric normalization models.

a) Endmember detection, pixel unmixing, and target detection targets.

This set of targets accounted for 60 of the targets constructed for this data collection. Three different size targets were used, 20 targets for each size, to account for the three general scales of objects that can be observed in a collection. The smaller size targets measured .5m x .5m, shown in Figure 4, and were used to simulate targets that were smaller than the spatial resolution of the hyperspectral sensor being used (1m x 1m). A medium size target measuring 1m x 1m, pictured in Figure 5, created a target that was the same size as the spatial resolution of the hyperspectral sensor. While it is possible that this target could create exactly one pure pixel, based on the area of the target and the pixel, it is not likely. In most cases this target will provide four adjacent pixels of varying target spectra abundances. The larger size target (3m x 3m), as pictured in Figure 6, will guarantee at least one pure pixel (excluding an occlusion by tree coverage).

Each of the 60 endmember detection target frames were constructed from 1"x2" and 2"x4" boards. The frames were then covered with 100% cotton fabric of varying colors, more details about the target material will be discussed in the following section. Twenty targets of each size where constructed, of those twenty targets four different color fabrics were used, each color covering 5 targets. Of the set of 5 targets from one color or each size, each were placed in positions of varying conditions and tree canopy coverage discussed in a later section. While a majority of targets where elevated to a height of 1.5 feet (demonstrated in Figures 4 and 5) some were laid at ground level (shown in Figure 6). This variety in target elevation will allow for a range of additional unmixing experiments utilizing elevation data from the LIDAR sensor.

Figure 2-4: Small elevated target (.5m x .5m) with Soil Brown fabric

Figure 2-5: Medium size elevated target (1m x 1m) with Vineyard Green fabric

Figure 2-6: Large size ground level target (3m x 3m) with Vineyard Green fabric

b) Atmospheric Modeling Targets

The targets constructed for the atmospheric models experiments account for four of the targets built. Each of these targets, shown in Figure 7, was ground level and measure 6m x 10m. None of the targets had any tree occlusion and each was a different color, as discussed in a later section. The size and placement of these targets ensured that the collection would contain several pure pixels of each of the targets.

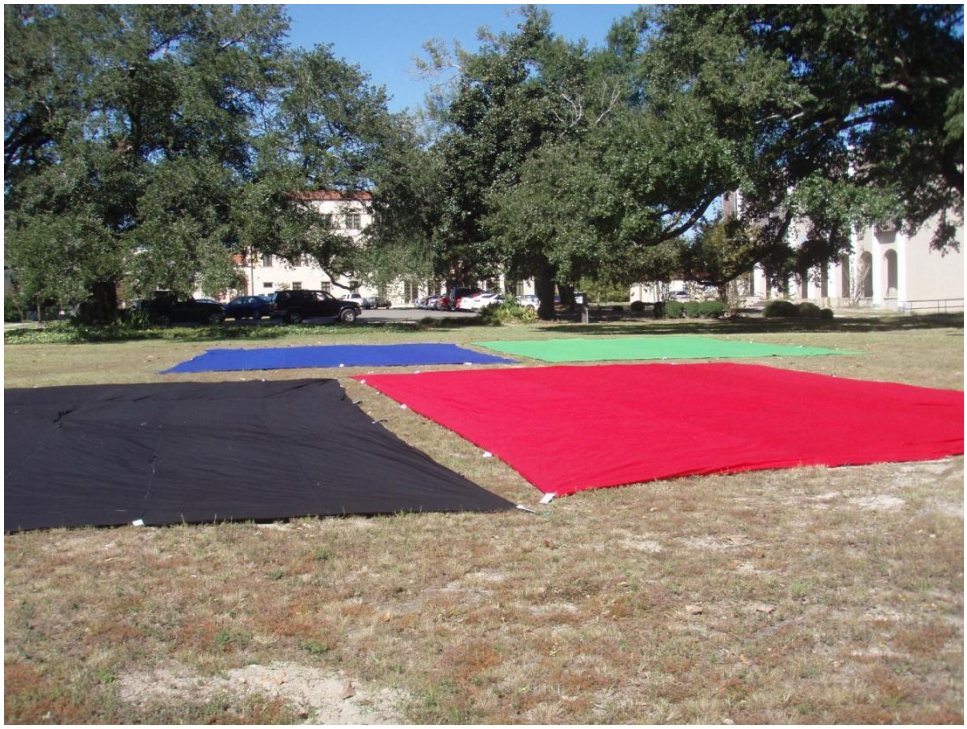

Figure 2-7: Atmospheric model evaluation targets

Once the number and spatial characteristics of the targets was determined, spectral characteristics were considered. The following two criteria were considered very important.

Lambertian Reflectance. To provide for accurate spectral ground truthing we needed targets that would exhibit the same spectral signature (holding all else constant) from all angles of view. This is necessary given the unpredictable and dynamic angle of collection from the aircraft. A Lambertian surface exhibits this property, i.e. regardless of the angle of observation the light reflected off the surface looks the same. This property therefore ruled out glossy paint, cloths, or other plastic materials as their shiny appearance indicated poor Lambertian reflectance.

Uniform Spectral Signature. To accurately estimate the effectiveness of a given unmixing algorithm a precise measurement of the target's spectra is needed. This spectra mixed with other objects present in the scene creates the mixed nature of the hyperspectral pixel. Uniformity in the spectral signature of the targets is needed to accomplish this. Therefore, after observing the difficulty in creating a uniform and opaque paint layer with matte finish, candidate targets that would require painting to alter their spectral signature were excluded (such as wood or cardboard).

After considering the above criteria it was decided to use 100% cotton fabric purchased from a local sewing shop. The fabric provides for a uniform spectral signature that closely approximates Lambertian reflectance. A total of eight different types of fabrics were purchased with varying spectral signatures; this was initially determined by visual inspection and with the use of a video camera. The video camera has sensitivity into the NIT region to allow it to operate in night shot mode. Four colors were chosen exclusively for the purpose of creating the atmospheric modeling targets discussed previously. The colors chosen for these targets were Bamboo Green, Red, Blue, and Black. This choice of colors gave us a wide spread of reflectance values within the visible spectrum in which to evaluate the atmospheric modeling. The remaining four colors chosen were used in the endmember detection targets. These colors were Solid Dark Green, Vineyard Green, Soil Brown, and Pea Green. The spectral signatures from samples of each of the 8 fabrics were then measured with a Cary500 spectrophotometer using 1nm resolution in the range of 200-2500 nm. Figure 8 shows the resulting signatures of the 8 fabrics in the visible (VIS)/ Near-IR (NIR) ranges.

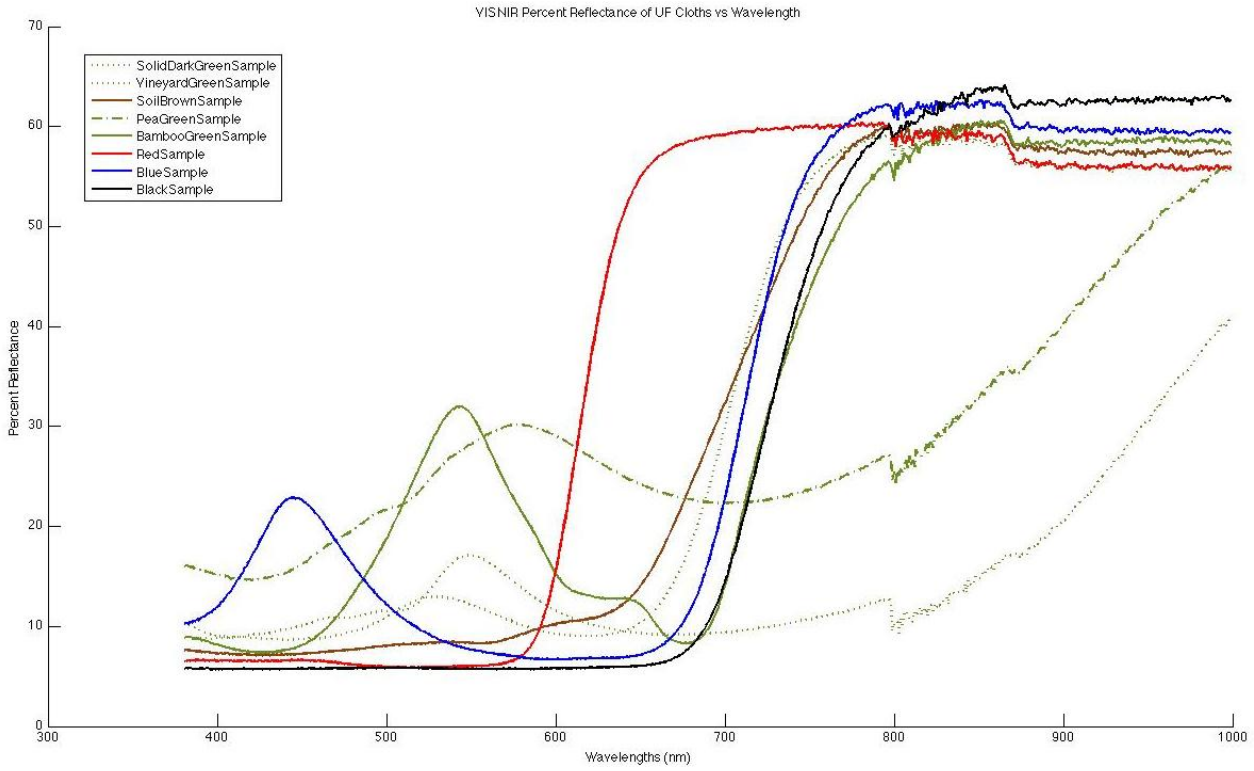

Figure 2-8: Spectral signatures of the eight target fabrics in the VIS/NIR range

In addition to choosing fabrics that presented a variety of colors in the VIS ranges, we also choose fabrics that presented various responses in the NIR ranges. As you can see from Figure 8, most fabrics have a very similar response in the NIR ranges of the EM spectrum. We were able to find two colors that presented lower reflectance in the NIR wavelengths, Vineyard Green and Pea Green. Vineyard green is shown in the graph from Figure 8 as the dotted line that has the lowest reflectance in the NIR ranges. As an additional note, when ordering the chosen fabrics a mistake was made with the Vineyard Green such that 1/5 of our fabric was the originally chosen fabric and 4/5 of the fabric was a different green. Due to time constraints we had to use the incorrect fabric which unfortunately has a similar NIR reflectance to the other fabrics. Consequently, the targets constructed for pixel unmixing experiments are constructed from 5 different fabrics.

2.3 Target Emplacement

Targets were emplaced so that there would be representatives of each color type (except the original Vineyard Green) completely non-occluded, partially occluded, and almost totally occluded. As a consequence, one can extract pure pixels of most of the colors but it is unlikely that any algorithm will be able to find all the targets. Target emplacements will be discussed more in the section on establishing ground truth.

2.4 Ground Measurements

Ground based spectral measurements were collected using two devices, the ASD and the DiveSpec. The ASD is a standard handheld spectrometer that measures radiance and reflectance. The DiveSpec is designed to be a submersible spectrometer but is also useful on land. The DiveSpec has an advantage in that it generates its own light source and can produce reflectance that is independent of the intervening atmosphere (or water body).

The spectrometers were used to measure a variety of ground surfaces, including sand, grass, asphalt, tree bark and leaves. Additionally the spectrometers measured the reflectance of the Atmospheric Modeling cloths, which were laid out on the Long Beach campus on November 8, 2010. Figure 3 shows the location of the Atmospheric Modeling cloths. These cloths were measured with the ASD and the DiveSpec during aircraft overflight on November 8, 2010.

More than 641 ground spectral measurements were taken with the ASD. Ground measurements were made on target cloths. The following measurements were taken from other objects in the scene.

Material	Number of Measurements
Asphalt	30
Bark	30
Sand	66
Wood Stairs on Beach	10
Building	70
Butterfly	20
Concrete	15
Dead Weeds	10
Dirt	5
Dried Leaves	6
Friendship Oak	50
Grass	13
Ground Litter	10
Land Hyacinth (Not sure about the name)	10
Leaves and Bark Mixed	80
Live Oak Bark	70
Live Oak Leaves	70
Pillar	20
Powder	10
Sidewalk	17
Yellow Curb	10

In addition to the ground spectral measurements, GPS information was recorded on the ground. Two GPS basestations were set up on November 8, one basestation at Stennis Airport in Kiln, MS and one basestation in the project area. Personnel from 3001, a

subcontractor to Optech, performed these measurements. To determine accuracy of the LIDAR a GPS Real Time Kinematic (RTK) survey was performed November 7 and 8, 2010 in the project area by 3001 Inc. The objective was to obtain high accuracy ground measurements (XYZ) of different terrain surfaces (bare earth, asphalt, concrete, grass) and compare them with the airborne measurements.

2.5 Airborne Measurements

Aircraft operations were based out of Stennis Airport in Kiln, MS, November 6 - 8, 2010 and were conducted by personnel from Optech International Inc. and their subcontractor, 3001 Inc.. The airborne instruments included an Optech Inc. Gemini Airborne Topographic LIDAR Mapper (ALTM) system, an ITRES Inc. hyperspectral Compact Airborne Spectrographic Imager (CASI-1500), and an Applanix Inc. Position and Orientation System Airborne Vehicle (POS/AV) navigation system installed in a King Air 200. All three instruments were integrated using the POS/AV GPS Pulse Per Second (PPS). The Gemini sensor head and the CASI-1500 sensor head were mounted on the same mounting plate (the Inertial Measurement Unit or IMU is located inside the LIDAR sensor head), shown in Figure 1. The configuration of the LIDAR and hyperspectral sensors is described in Table 1 and 2.

Installation and initial test flight took place November 6. A boresight flight for the hyperspectral camera was conducted November 7, 2010 over the town of Diamondhead, MS. The main project area, was flown on November 8, 2010. During this flight boresight calibration lines were collected for the LIDAR system. Weather for all three days was very clear with minimal haze. Water clarity on November 8 was relatively clear for this area.

Data collection over Long Beach took place on November 8, 2010 from 11:15 am to 12:20 pm under clear skies. Solar noon was approximately 11:45 am. More specifically, there were five collection flights over the site. Three of the flights were at an altitude of 3500 feet and two of the flights were at 6700 feet. Both hyperspectral and LIDAR data were taken on the two of the three lower altitude flights. Only hyperspectral data were taken on the higher altitude flights. There were also two flights taken for navigational purposes at headings of 180 and 0 degrees. These details are summarized in the following table.

Table A-1 Summary of delivered hyperspectral CASI and Gemini LIDAR data for November 8, 2010.

Local time	CASI raw filename	LIDAR filename	Altitude (ft AGL)	Heading (°)
11:27 AM	CASI_2010_11_08_112759	Line002.las	3500	90
11:35 AM	CASI_2010_11_08_113534	Line001.las	3500	90
11:40 AM	CASI_2010_11_08_114028		3500	270
11:47 AM		Line003.las	3500	180
11:51 AM		Line004.las	3500	0
11:58 AM	CASI_2010_11_08_115837		6700	90
12:06 PM	CASI_2010_11_08_120618		6700	90

The system was uninstalled on November 9, 2010.

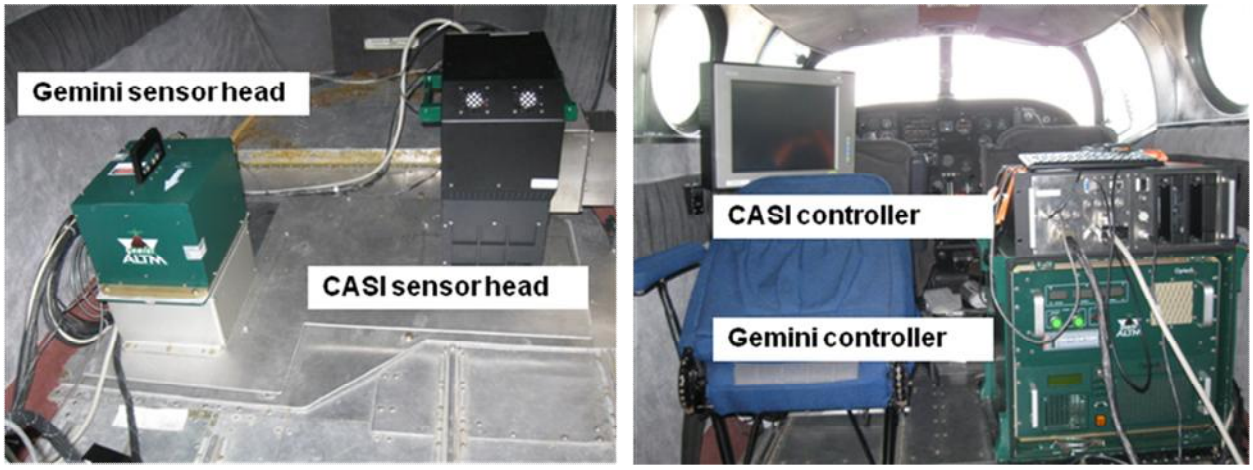

Figure 1 View towards aircraft tail showing the Gemini LIDAR and CASI-1500 hyperspectral sensor heads (left) and view towards aircraft nose showing instrument controllers and hyperspectral operator monitor (right).

Table 1 Configuration of the Gemini ALTM LIDAR system.

Optech Gemini Airborne Terrain Laser Mapper (ALTM)	
Laser λ	1064 nm
PRF	70 KHz
Scan frequency	43 Hz
Scan angle	30°
Swath width at 3500' AGL	489 m
Spot spacing	0.60 m across track 0.78 m along track
Recorded	First, Second, Last return

Table 2 Configuration of the CASI-1500 hyperspecctral imager.

ITRES CASI-1500		
λ range	375 – 1050 nm	
# of spectral bands	72	
Bandwidth	10 nm	
Spatial res @ 3500' AGL	0.54 m across track m along track	1.0
Swath width @ 3500' AGL	795	

2.6 Post-Processing

2.6.1 LIDAR Processing

LIDAR data were processed by 3001 Inc. Raw data were processed in the Optech Inc. DASHMap software to generate American Society of Photogrammetry and Remote Sensing (ASPRS) LASer (LAS) format files. The TerraSolid Ltd. software TerraScan and TerraMatch were used to find misalignments between the IMU and the User Frame (LIDAR mirror). Finally, GPS ground control points were used to validate the vertical fit.

The horizontal datum of the LIDAR data is NAD83 and the vertical reference is NAVD88 based on application of the GEOID09 model.

LIDAR quality assurance (QA) information was measured by 3001 Inc.. After comparison with 191 GPS data points collected over a variety of surfaces, the accuracy of the LIDAR is reported as Vertical Root Mean Square Error of 0.05 m. The mean elevation difference for all points is -0.03 m. Standard deviation reported as 0.04 m for 184 GPS points.

2.6.2 Hyperspectral Processing

CASI-1500 hyperspectral data processing was performed by Optech. It consisted of standard radiometric and geometric corrections to produce image maps using ITRES Inc. software. Laboratory measurements taken with the sensor head in a calibrated integrating

sphere provided correction coefficients to convert Digital Numbers (DN) to calibrated Spectral Radiance Units (SRU) where 1 SRU = 1 μW / cm^2 sr nm. The first step in hyperspectral image processing involved applying the correction coefficients to the raw airborne data to convert to SRU. The next step involved synchronizing the hyperspectral scan lines with the POS/AV position and orientation measurements, primarily relying on the GPS PPS. Once the XYZ, roll, pitch, heading measurements were tagged for each hyperspectral scan line a geocorrected image map was produced. To co-register with the LIDAR, the geocorrected image at the native spatial resolution (in figure xxx) was mapped to a 1m x 1m spatial resolution image using a nearest neighbor mapping. That is, the specgturm assigned to each location in the 1m x 1m grid (defined by GPW coordinates the spectrum measured at the closest GPS coordinate in the native spatial resolution. This method has the disadvantage that some measurements in the native spatial resolution image may not be assigned to any 1m x 1m grid cell and the advantage that only measured spectra are present in the 1m x 1m image. Averaging would produce spectra that were never measured but all measured spectra would contribute to at least one 1m x 1m grid cell.

After image maps were produced two atmospheric corrections were performed: an Empirical Line Method based on situ ASD measurements and a model-based atmospheric removal program from the Optech International Rapid Environmental Assessment (REA) software.

The ELM utilized ASD spectra of sand and the asphalt roadway. The ENVI ELM algorithm compared CASI-1500 radiance spectra of the sand and asphalt with the ASD spectra and computed the scene irradiance and path radiance which were removed from the radiance image to produce surface reflectance.

The REA model approach relies on calculating the total downwelling irradiance at the earth surface using a solar irradiance model. Remote sensing reflectance is calculated using the definition

$$R_{rs} = L / E_d ,$$

where L is radiance and E_d is downwelling irradiance, and the remote sensing reflectance will have the unit of [1/sr]. The solar irradiance is obtained using SMARTS (Simple Model of the Atmospheric Radiative Transfer of Sunshine) model by NREL (National Renewable Energy Laboratory). In the computation of solar irradiance the SMARTS model requires several parameters, such as (1) atmospheric condition (2) UTC time (3) latitude and longitude. In this case, atmospheric conditions were not measured; average atmospheric conditions were used. Specifically, "mid-latitude atmosphere with maritime aerosol model" was used. According to the sensitivity analysis by varying different atmospheric conditions, total downwelling irradiance is relatively insensitive. As the atmosphere changes from clear to hazy condition, relative contribution by the diffuse sky irradiance and direct solar beam irradiance changes. However, the total downwelling irradiance as the sum of both components remains pretty constant with negligible difference. Spectral

shape in the blue region is more sensitive than other regions. However, except for very hazy conditions, the difference is minimal.

One problem that is apparent in the strong water vapor absorption band near 940 nm is that the incorrect guess of column water vapor amount will strongly enhance the reflectance conversion error. Generally speaking, the radiance at 940 nm is relatively small compared to the neighbor wavelengths due to the water vapor absorption. Thus, if the column water vapor input to the SMARTS model is greatly different than the real condition, the calculated reflectance will have big error when the CASI radiance is divided by the incorrect irradiance at 940 nm. It can be solved by iterative optimization of column water vapor. However, we did not implement the algorithm in the current data processing.

Comparison of reflectance spectra from the two methods with ground based measurements are shown next.

The first step to analyzing airborne spectral reflectance is to determine reliable ground based reference spectra. We compared the Carys 500 lab spectrometer tarp reflectance to the ASD spectra collected on the Long Beach campus November 8, shown in Figure 5. In the red and blue tarp reflectance we see the ASD spectra exceed 100% reflectance, indicated a change in illumination or viewing angle between the white panel scan and the tarp scan.

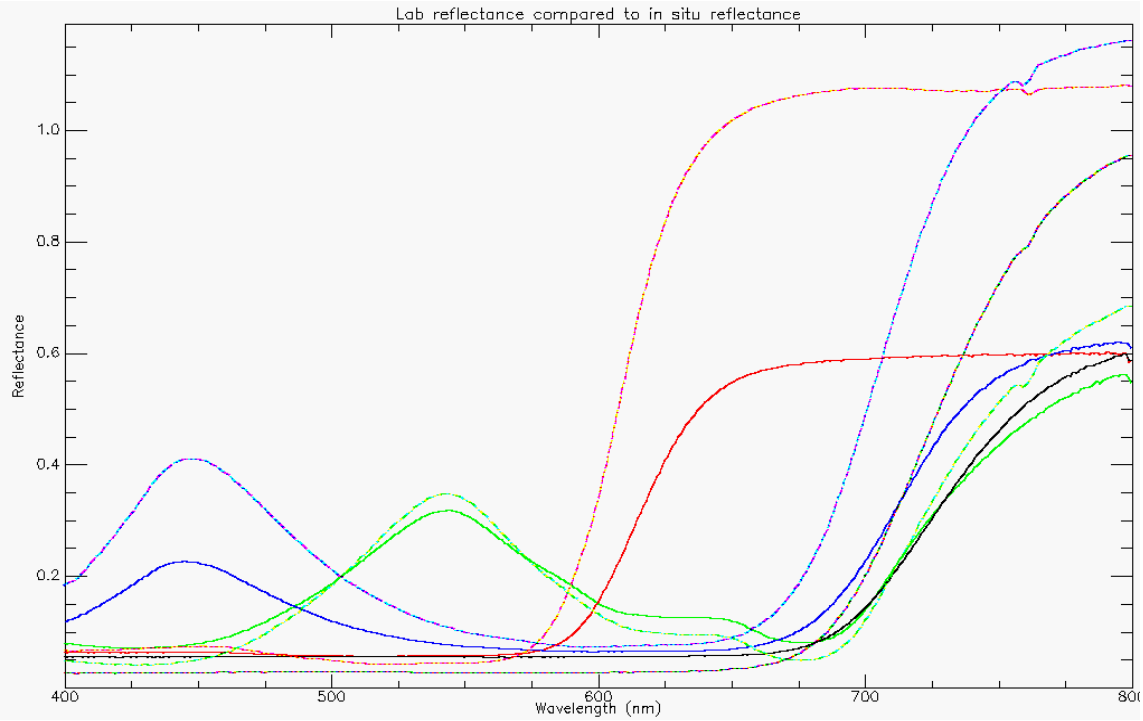

Figure 5 Tarp reflectance collected with a Carys 500 lab spectrometer (solid lines) and ASD in situ (dotted lines).

Next we compare reflectance spectra extracted from the airborne atmospherically corrected CASI-1500 hyperspectral imagery to the ground based spectra. For this comparison we selected the Carys-500 lab reflectance. Figures 6, 7, 8, and 9 show reflectance spectra for the red, green, blue and black tarps, respectively. The spectra from the CASI corrected with the atmospheric model show abnormally high reflectance at 940 nm; this is an error in the model's calculation of the amount of atmospheric water vapor determined from the 940 nm atmospheric absorption feature. Otherwise, both sets of CASI-1500 data agree favorably with eachother and with the lab-measured spectra.

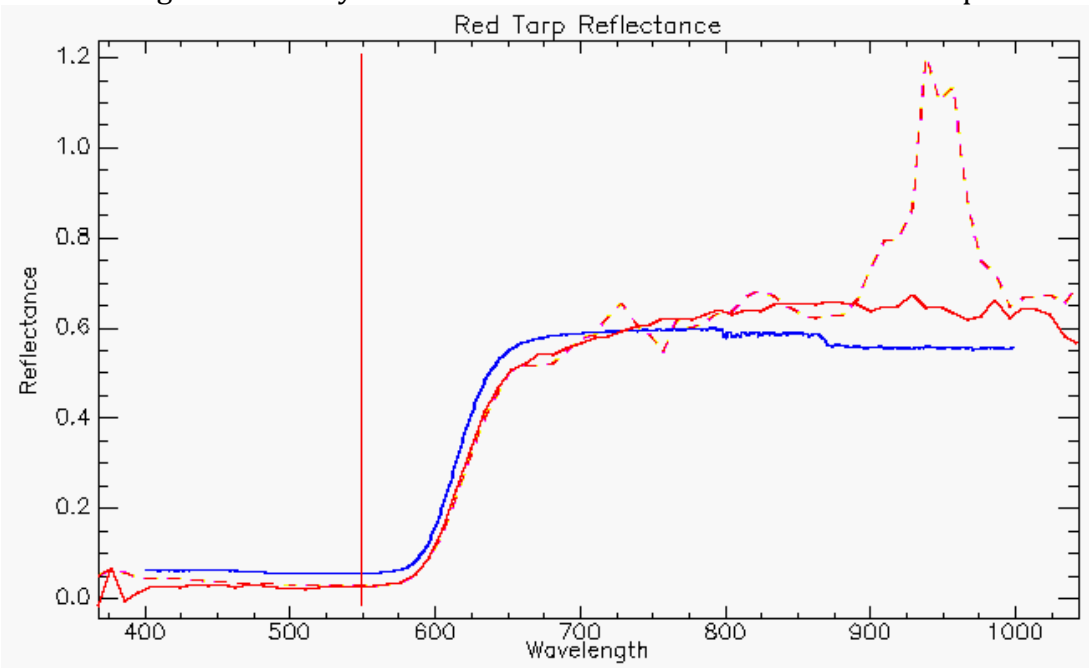

Figure 6 Comparison of red tarp reflectance: Carys 500 lab reflectance (blue solid line) compared CASI ELM result (red solid line) and CASI modeled atmospheric correction result (red dashed line).

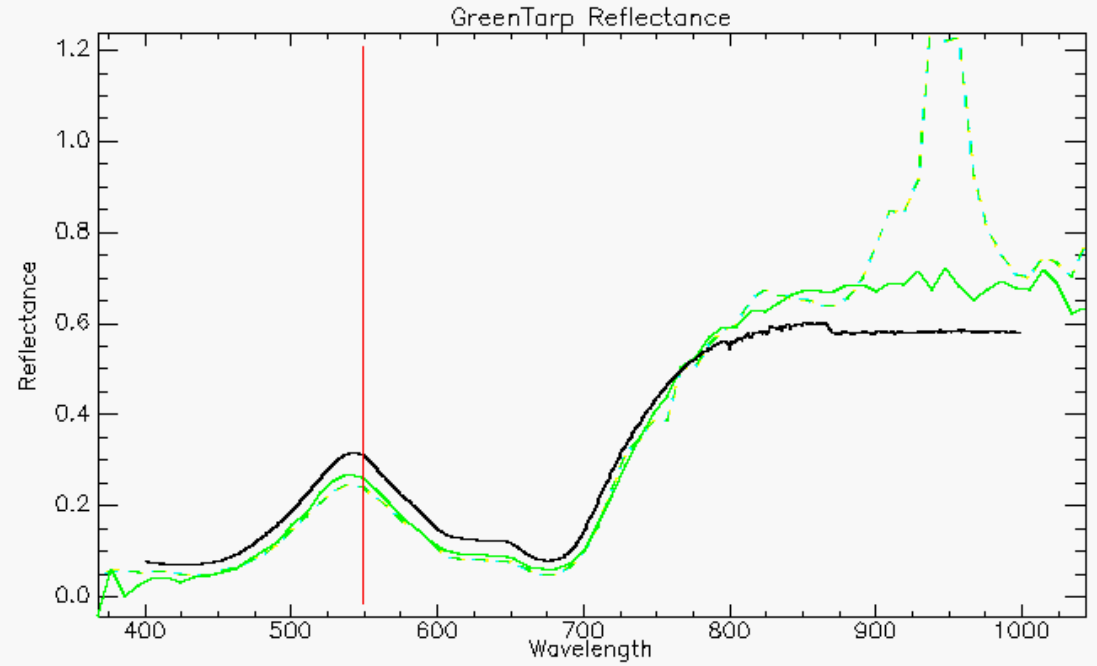

Figure 7 Comparison of green tarp reflectance: Carys 500 lab reflectance (black solid line) compared CASI ELM result (green solid line) and CASI modeled atmospheric correction result (green dashed line).

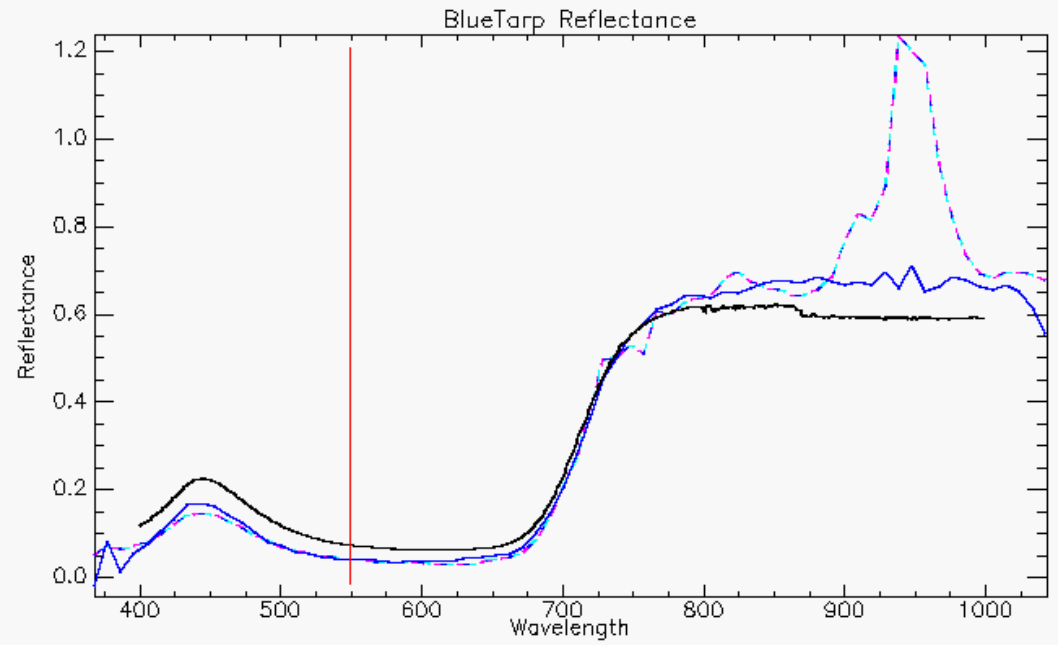

Figure 8 Comparison of blue tarp reflectance: Carys 500 lab reflectance (black solid line) compared CASI ELM result (blue solid line) and CASI modeled atmospheric correction result (blue dashed line).

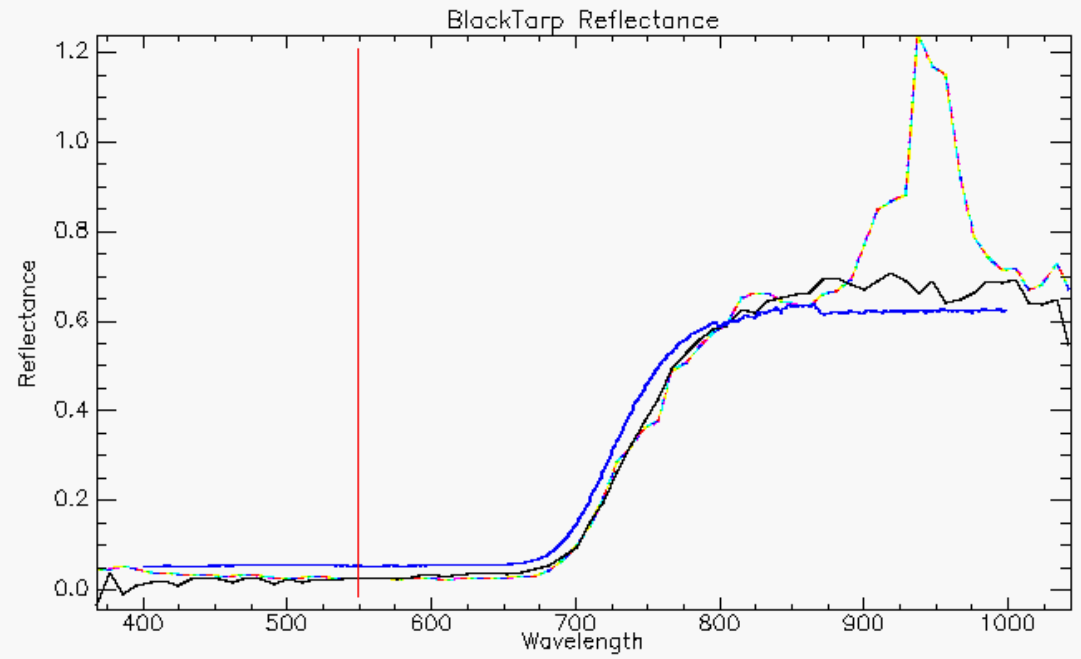

Figure 9 Comparison of black tarp reflectance: Carys 500 lab reflectance (blue solid line) compared CASI ELM result (black solid line) and CASI modeled atmospheric correction result (black dashed line).

Based on these results, the ELM estimated reflectance has been used. A summary of data that were delivered by Optech to the University of Florida, is given in Appendix A.

2.7 Ground-truthing

The last step in the data collection activity is assigning ground-truth. Ground-truth involves identifying the pixel locations in the various images at which the cloth targets and some of the other objects appear to be located. This is an important step so that any experiments that are conducted have as accurate answers as possible. It is also a difficult step for several reasons: the inherent uncertainty in GPS locations measured by both the airborne and ground-based instruments, the difficulty of visually identifying highly occluded targets in the scene, and the difficulty of visually identifying sub-pixel targets in the scene.

The image data that were delivered by Optech to the University of Florida included GPS coordinates of the pixels and LIDAR points. These coordinates were assigned as described above. In addition, GPS coordinates were measured on the ground at all emplaced target locations and at locations of many other objects. These coordinates were measured with a Trimble Juno SB hand-held GPS that was on loan from Trimble. These devices have an error of 2-5 meters. Several coordinates were actually measured at each target location by turning on the device and walking a complete loop around the target.

The ground-truthing involves taking the set of GPS coordinates measured by the hand-held GPS and mapping them to a pixel location in each image. The straightforward method of doing this would be to take the average of the ground GPS measurements and then finding the pixel in each image with the closest airborne GPS measurements. However, this method would not produce very accurate ground truth due to the errors in the measurements. The method was used as the baseline, or default, method, and will be referred to as such later. Therefore, interactive GUIs were created using MATLAB to help produce more accurate ground truth locations; one GUI was used for hyperspectral and the other for LIDAR. The GUIs went through several design iterations before assuming their final form.

The hyperspectral GUI allowed the user to go through subimages of the hyperspectral images one by one. Each subimage contained a cloth target and some background. There were subimages for all 5 swaths. For each cloth target, there were 4 screens corresponding to the region in the subimage. One screen showed the output of a detector designed for this purpose. The detector worked by unmixing pixels with respect to target and background endmembers. The output was the proportion associated with the target. The target endmember was selected from the 3m x 3m target in the scene since a pure pixel was guaranteed on those targets. The background endmembers were defined to be the pixels in the neighborhood of each pixel. This detector, which can be thought of as a running unmixing detection algorithm, performed better than several other that were tried.

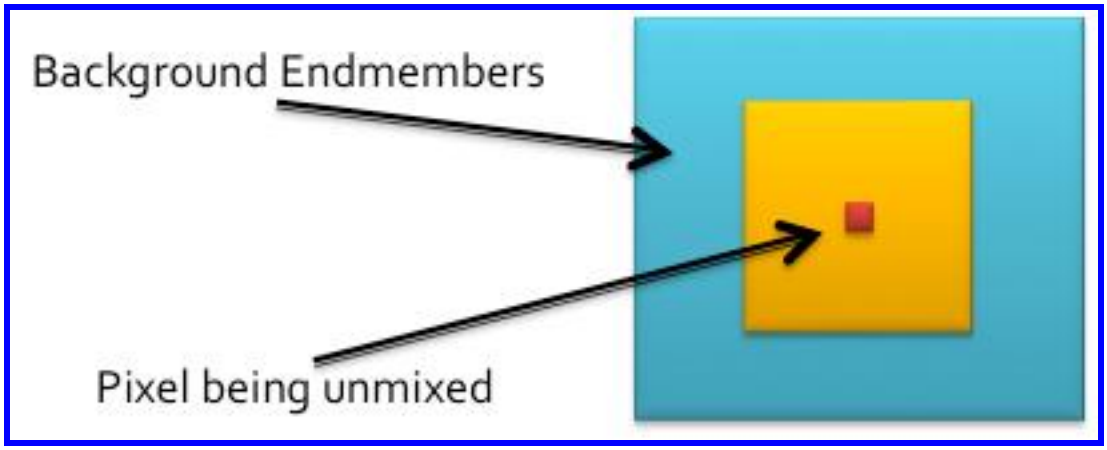

Figure 10. Depiction of detector used to help ground-truth targets. The center pixel (in red) was unmixed (using fully constrained quadratic programming) with respect to a specific target pixel and background endmembers consisting of neighboring pixels. The output at the center pixel was the proportion of the pixel assigned to the target endmember. The detector was run at every point in a subimage containing the location of the specific target.

Another screen depicted the RGB image of the scene derived from the subimage. LIDAR images are shown in the other screen. Various mouse tools were developed to interrogate pixels and display their spectral content. It turned out that if a target accounted for a "significant" percentage of the reflectance of a pixel, then one could see the spectral shape of the target in the spectral pixel at that location. Therefore, one could fairly confidently assign GPS coordinates to some pixels that were not pure. The LIDAR provided context in

terms of elevations of objects around the target location. A typical screen is shown in Figure 10. The default location is marked with a white × in the RGB, Proportion Map, and LIDAR displays. On careful inspection, one can see that the target is a 3m x 3m target partially occluded under the oak tree canopy. The detection location is a few pixels from the default GPS location. Furthermore, the spectrum at the detection location looks quite good compared to measure spectra for that target. Therefore, the ground truth location would be modified from the default location to the one indicated by the detector output.

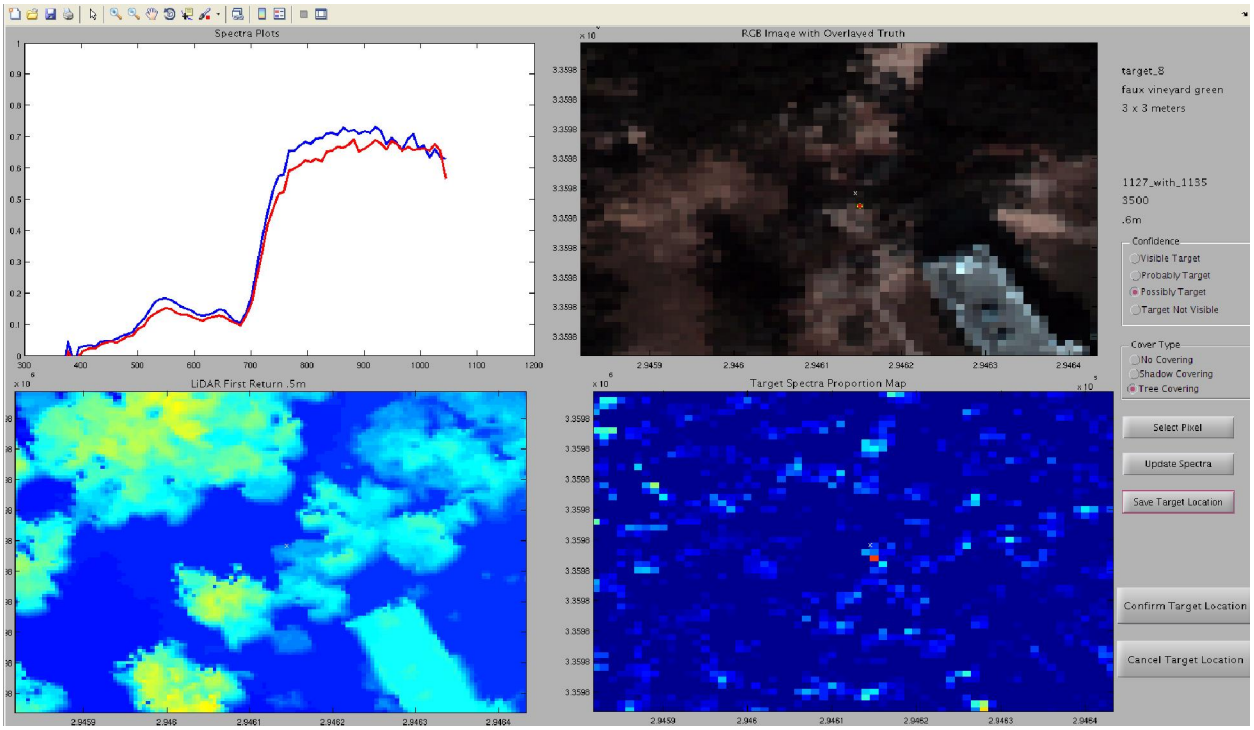

Sometimes there were no indications of targets in any of the data. In such a case, the default location was used. A refined procedure was developed for using the interface with all the screens and detector outputs to assign ground truth locations for each target and also to assign a subjective confidence in our assignment and a category. The values were as follows:

Confidence numbers:
1 - Visible
2 - Probably the target
3 - Possibly the target
4 - Target not visible

Cat. (Category)
0 - Target not covered (i.e. no shadow and no tree occlusion at all)
1 - Covered partly or fully with shadow but no tree
2 - Part or all of the target is covered by a tree branch (and by assumption probably shadow as well)

After a few design iterations, the hyperspectral ground-truth activity procedure was determined to be as follows.

```
For each of the 60 emplaced targets
      For each of the 5 hyperspectral images
         ▪ GUI selects subimage on the default GPS location
         ▪ Viewers evaluate the displays and try to determine the most
           likely truth location, confidence, and category using the screens
           displayed by the GUI
         ▪ If the target is not visible, the default GPS location is used
      EndFor
EndFor
```

This procedure produces a ground-truth location, confidence, and category for each target and each image. There are therefore 5 x 60 = 300 such sets of values. These values are stored in a .csv file and will be made available. A similar procedure was developed for LIDAR alone and an analagous .csv file has been created.

The final step in the ground-truthing process involved entering the information into Google Earth. A Google Earth file (.kml format) was constructed that incorporated photographs and other information at the assigned ground-truth locations and at assigned locations of some of the other objects in the scene. A total of 301 images are associated with the .kml file. If one opens the .kml file, the campus will be shown in Google Earth with "pins" or "markers" for each location. There are pins or markers showing the approximate locations of targets in the scene, of some of the spectral collections taken on the ground in the scene, and of other objects in the scene. There are also pins showing the locations of where photographs were taken in the scene. They are color-coded and size-coded. There is a different color marker for each of the nine targets colors. In addition, different size targets have different size markers.

If one clicks on those pins or markers, one can observe photograph(s) taken at that approximate location, In addition, there are many other photographs of the scene that have not been associated with ground locations. Note, Google Earth will behave strangely if the computer is not connected to the internet.